ChemPubSoc Europe
DOI: 10.1002/open.201500207
Open Access ChemistryOPEN Reviews

Oxyhydroxy Silicate Colloids: A New Type of Waterborne Actinide(IV) Colloids

Harald Zänker,* Stephan Weiss, Christoph Hennig, Vinzenz Brendler, and Atsushi Ikeda-Ohno[a]

At the near-neutral and reducing aquatic conditions expected in undisturbed ore deposits or in closed nuclear waste repositories, the actinides Th, U, Np, and Pu are primarily tetravalent. These tetravalent actinides (An^{IV}) are sparingly soluble in aquatic systems and, hence, are often assumed to be immobile. However, An^{IV} could become mobile if they occur as colloids. This review focuses on a new type of An^{IV} colloids, oxyhydroxy silicate colloids. We herein discuss the chemical characteristics of these colloids and the potential implication for their environmental behavior. The binary oxyhydroxy silicate colloids of An^{IV} could be potentially more mobile as a waterborne species than the well-known mono-component oxyhydroxide colloids.

1. Introduction

Uranium (U) and thorium (Th) are the two actinides which occur as natural constituents of the earth's crust; they are ubiquitous on earth. Due to their chemical toxicity and radiotoxicity, they pose potential risks to human life. They might cause, for instance, problems with drinking water supplied from the former mining areas or for some commercial mineral waters.[1,2] On the other hand, U and Th are also precious natural resources with economic importance, namely for nuclear power generation. There, problems are associated not only with the legacy of ore mining activities but also with the safe storage of nuclear waste. The nuclear wastes in the latter case contain significant fractions of the original fuel (i.e., U) with additional fractions of highly radioactive actinides such as neptunium (Np) or plutonium (Pu) all of which could be present in the tetravalent form (i.e., An^{IV}) in natural aquatic systems. The potential release of these actinides from nuclear waste repositories into groundwater would cause serious environmental concerns.[3–12]

In strongly acidic solutions, An^{IV} species are soluble. However, due to their strong hydrolysis, they tend to form oxyhydroxide oligomers, polymers, and colloids when pH increases.[13–24] A variety of dimers, trimers, higher oligomers, and nanoclusters can be generated just below the pH where precipitation occurs.[25–31] The oligomers and clusters are often stabilized by coexisting ligands such as Cl^- or carboxylates which act as growth-terminating bridging ligands, preventing the clusters from further polymerization and aggregation in solution.[27,31–39] Figure 1 gives an example. It shows the nano-sized Pu oxide cluster, $[Pu_{38}O_{56}]^{40+}$, which is decorated with 54 Cl^- to form $[Pu_{38}O_{56}Cl_{54}(H_2O)_8]^{14-}$, and which shows a high stability even in aqueous solutions.[27]

Slightly above the pH where precipitation occurs, colloids appear. According to the definition by the International Union of Pure and Applied Chemistry (IUPAC), colloids are waterborne particles with the size of 1 nm to 1 μm, at least in one dimension. In the case of oxidic An^{IV} colloids, such colloids are often regarded as amorphous An^{IV} oxyhydroxide nanoparticles. However, a closer look into these "amorphous" oxyhydroxides by high-resolution transmission electron microscopy (HR-TEM) has revealed that these colloids are composed of nanocrystalline domains of the fluorite-analog uraninite type ($Fm\bar{3}m$)[40–44] which also refers to the oxyhydroxide of Zr^{IV}, a chemical analog

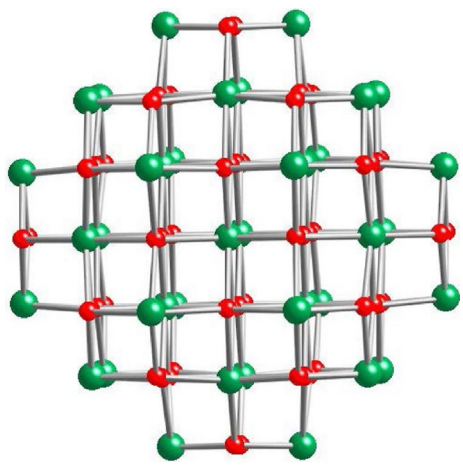

Figure 1. Structure of the $[Pu_{38}O_{56}]^{40+}$ core in the $[Pu_{38}O_{56}Cl_{54}(H_2O)_8]^{14-}$ cluster which is stable even in aqueous solutions. Reproduced with permission from Ref. [31]. Copyright 2013, American Chemical Society.

[a] Dr. H. Zänker, S. Weiss, Dr. C. Hennig, Dr. V. Brendler, Dr. A. Ikeda-Ohno
Institute of Resource Ecology, Helmholtz-Zentrum Dresden-Rossendorf
P.O. Box 51 01 19, 01314 Dresden (Germany)
E-mail: h.zaenker@hzdr.de

© 2016 The Authors. Published by Wiley-VCH Verlag GmbH & Co. KGaA. This is an open access article under the terms of the Creative Commons Attribution-NonCommercial License, which permits use, distribution and reproduction in any medium, provided the original work is properly cited and is not used for commercial purposes.

of An^{IV}.[45] These An^{IV} oligomers and clusters are dissolvable in aqueous solutions as waterborne colloids, which also exhibit the $Fm\bar{3}m$ structure.[27,37] Similar waterborne colloids can be observed also for Ce(IV), another chemical analog of An^{IV}.[46]

The colloid chemistry of An^{IV} oxyhydroxide nanoparticles formed in the acidic to near-neutral pH range can be summarized as follows:

i) **At very low pH**. An^{IV} species exist in truly dissolved forms such as An^{4+}, oligomeric, and small polymeric species.
ii) **At low pH**. An^{IV} species occur as colloids when pH slightly increases. In this pH range, An^{IV} oxyhydroxide colloids are stable in the waterborne form at concentrations of tens of mM over months.[47,48]
iii) **At near-neutral pH, major An^{IV} fraction**. When pH increases further, a large proportion of An^{IV} oxyhydroxide colloids precipitates. This is in line with the Derjaguin, Landau, Verwey, and Overbeek (DLVO) theory. An^{IV} oxyhydroxide colloids possess isoelectric points (IEPs) of pH 5 to 9,[49–52] and it is obvious that, as soon as the pH reaches the near-neutral region, the electrostatic repulsion is no longer sufficient to stabilize the particles, causing coagulation.
iv) **At near-neutral pH, minor An^{IV} fraction**. There is, however, a small fraction of these colloids which exist in a waterborne form even at the near-neutral pH. For instance, Th^{IV} is able to form such colloids over a wide pH range above pH 6, resulting in the formation of colloid-borne Th^{IV} with a concentration of $\sim 10^{-6}$ M (Figure 2).[11,13,53] These colloids of An^{IV} oxyhydroxide are often regarded as amorphous and can be described as being in equilibrium with the dissolved actinide species, behaving as large ionic species. Hence, they do not obey the DLVO theory.[11,15,17,54] The formation of these colloids increases the concentration of waterborne An^{IV} by several orders of magnitude as compared with their thermodynamically expected solubility,[53] which could pose a concern for the safety assessment of nuclear waste repositories.

Harald Zänker received his diploma at the Dresden Technical University in 1977. While working in the Rheinsberg Nuclear Power Plant, he did research on defective fuel rod detection based on radionuclides in the coolant. He received his Ph.D. degree at the Central Institute of Nuclear Research Rossendorf in 1986. In the nineties, he established a group for environmental colloids at the Institute of Radiochemistry of the Helmholtz Center Dresden-Rossendorf. In 1994 he worked as a visiting scientist with Prof. Robert J. Silva at the Lawrence Livermore National Laboratory. He was member of the former International Working Group "Aquatic Nanoscience & Nanotechnology" of the German Water-Chemical Society and is the co-author of more than 150 scientific publications and technical reports and of five patents. His current research interests include colloids of actinides and other radionuclides. Since his retirement in 2014, he continues research as a scientific consultant.

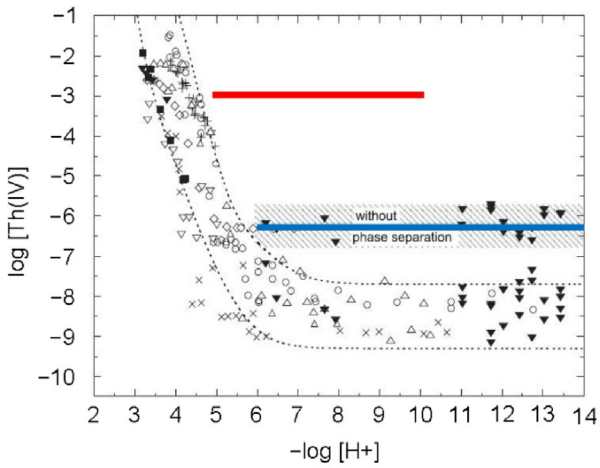

Figure 2. Solubility of amorphous Th^{IV} hydroxide or hydrous oxide at I = 0.1–0.6 M and 17–25 °C. Symbols: ◇ 0.1 M $NaClO_4$, × 0.1 M $NaClO_4$, + 0.1 M NaCl, ○ 0.5 M $NaClO_4$, △ 0.6 M NaCl, ▽ 0.5 M $NaClO_4$, ▼ and ■ 0.5 M NaCl (see Ref. [53] and references therein). The dashed curves represent the lower and upper limits calculated from the solubility product and hydrolysis constants discussed in Ref. [13]. The symbols in the shaded area show thorium concentrations measured without removal of colloids; the average of these values is given by the blue line which represents the "equilibrium concentration" of Th^{IV} oxyhydroxide colloids. The red line indicates the concentration of waterborne Th^{IV} oxyhydroxy silicate colloids reported in Ref. [52]. The red line does not provide an upper limit of the colloid concentration, but even higher concentrations of An^{IV} oxyhydroxy silica colloids could be expected. Reproduced with permission from Ref. [53]. Copyright 2004, De Gruyter.

It is obvious that there are no general sharp borders between regions (i) through (iv) because the hydrolysis constants differ for the different An^{IV} species and because the hydrolysis equilibria depend on the An^{IV} concentration. In the case of Th^{IV}, assuming a Th concentration of 10^{-3} M, region (ii) begins at roughly pH 2,[55] and regions (iii) and (iv) start at around pH 3 to 4.[15] In particular, it is difficult to clearly define the borderline between regions (i) and (ii). We would see the limit between regions (i) and (ii) when the colloids could be detectable by laser-induced breakdown detection (LIBD), a technique for particle/colloid characterization with an extremely low concentration detection limit of ppb down to ppt[56] and a particle size detection limit of 2 to 10 nm.[15]

In addition to An^{IV} oxyhydroxide colloids, a variety of other types of actinide colloids and nanoparticles have been investigated, for instance, peroxide colloids,[57] polyoxomethalate colloids,[58,59] or oxidic nanotubes.[60] However, An^{IV} oxyhydroxide colloids are probably the most studied type of actinide colloids/nanoparticles. These colloids have been investigated under well-controlled laboratory conditions that do not necessarily reflect the environmentally relevant conditions. For instance, groundwater contains a wide variety of ionic species, such as silicic acid with concentrations of 10^{-5} to 10^{-3} M.[61] The aim of this review is to shed more light on other types of An^{IV} colloids which are more environmentally relevant.

This review focuses particularly on the oxyhydroxy silicate colloids of An^{IV}. These colloids contain both An^{IV} and Si in the same colloid matrix via the reaction of dissolved An^{IV} with dissolved silicic acid. "Pseudocolloids" formed by the adsorption

© 2016 The Authors. Published by Wiley-VCH Verlag GmbH & Co. KGaA, Weinheim

of An^{IV} onto the surface of preexisting silica particles are not considered in this review. The formation of An^{IV} silicate colloids should have been anticipated given the existence of An^{IV} silicate minerals in nature, such as coffinite, thorite, huttonite, etc. Furthermore, Zr^{IV} is known to form oxyhydroxy silicate nanoparticles which are composed of Zr–O–Si direct bonds,[62] suggesting the possible formation of similar types of colloids for An^{IV}. Some trivalent metal cations, such as Fe^{III}[63–65] and Cm^{III},[66] are also known to form silica-containing oxyhydroxide colloids if precipitated in silicic acid solutions, reinforcing the potential formation of An^{IV} oxyhydroxy silicate colloids. In addition to a natural abundance of silicate species in groundwater, silicic acid has sometimes even been added to waters for drinking water treatment to "sequester" (make invisible) Fe^{III} in a colloid-borne form in order to prevent drinking water turbidity without removing the Fe^{III} by taking advantage of its tendency to form stable colloids with silicic acid.[63,64] Despite this knowledge found in the hitherto literature, the existence of An^{IV} oxyhydroxy silicate colloids has only recently been reported. This short and concise review will provide a summary of the recent findings on the An^{IV} oxyhydroxy silicate colloids and their potential implication for environmental concerns.

2. Generation of Actinide(IV) Oxyhydroxy Silicate Colloids

An^{IV} oxyhydroxy silicate colloids can be produced relatively easily, as described in Refs. [51], [52], and [67]. Starting solutions of An^{IV} carbonate complexes could be prepared by:

- Electrochemical reduction of U^{VI} carbonate complexes to the U^{IV} complexes,[51]
- Electrochemical reduction of Np^{V} to −(IV) in acidic solution and mixing the resultant Np^{IV} solution with $NaHCO_3$ solutions,[67] or
- Dissolution of Th^{IV} in $HClO_4$ and mixing with solid $NaHCO_3$.[52]

The experiments with U and Np need to be done in an inert atmosphere. The oxidation state of U and Np can be confirmed by UV/Vis spectroscopy.[51,67] Dilution of aqueous carbonate solutions of Th^{IV}, U^{IV}, and Np^{IV} with pure water typically results in the formation of An^{IV} oxyhydroxide colloids which tend to precipitate when the An concentration is high, while the dilution with silicic acid solutions yields stable suspensions of waterborne An^{IV} oxyhydroxy silicate colloids.[51,52,67] Silicic acid solutions can be prepared by the hydrolysis of tetramethyl orthosilicate (TMOS), $Si(OCH_3)_4$. No colloids which are filterable with 3 kDa molecular weight cut-off (MWCO) both in the An^{IV} stock solutions and in the silicic acid solutions were found in the experiments of Refs. [51, 52, and 67]. No Tyndall effect was observed in these two solutions, at least before mixing them. If necessary, the pH was adjusted with $HClO_4$ in these tests after mixing the solutions. Experiments were carried out below and above the so-called "mononuclear wall" of sicic acid of 2×10^{-3} M. This "wall" is the concentration limit above which the formation of silicic polymers is expected.[68] Differentiation between monosilicic acid and polysilicic acid is important since the affinity of polysilicic acid to metal ions is much stronger than that of the monosilicic one.[69,70]

3. Properties of Actinide(IV) Oxyhydroxy Silicate Colloids

3.1. Particle Size

Samples containing An^{IV} oxyhydroxy silicate colloids were centrifuged at different centrifugal accelerations between 10,500 and 170,000 g. Well-defined volumes of the centrifugates (the upper 50% of the supernatant volume) were carefully removed from the centrifuge tubes, and these supernatants were analyzed by inductively coupled plasma mass spectrometry (ICP-MS) and/or atomic absorption spectroscopy (AAS). Further details on this method of serial ultracentrifugation, which intends to avoid stirring up the particles concentrated in the lower part of the centrifugal tube, can be referred to in Refs. [51] and [71]. In parallel, ultrafiltration using disposable filtration units with molecular weight cut-offs of 1 to 1000 kDa were performed, and the filtrates were analyzed by ICP-MS and/or AAS. The samples, sample centrifugates, and sample filtrates were also investigated by light scattering.

Figure 3 shows the U concentration, the Si concentration, and the intensity of scattered light (originated in Tyndall

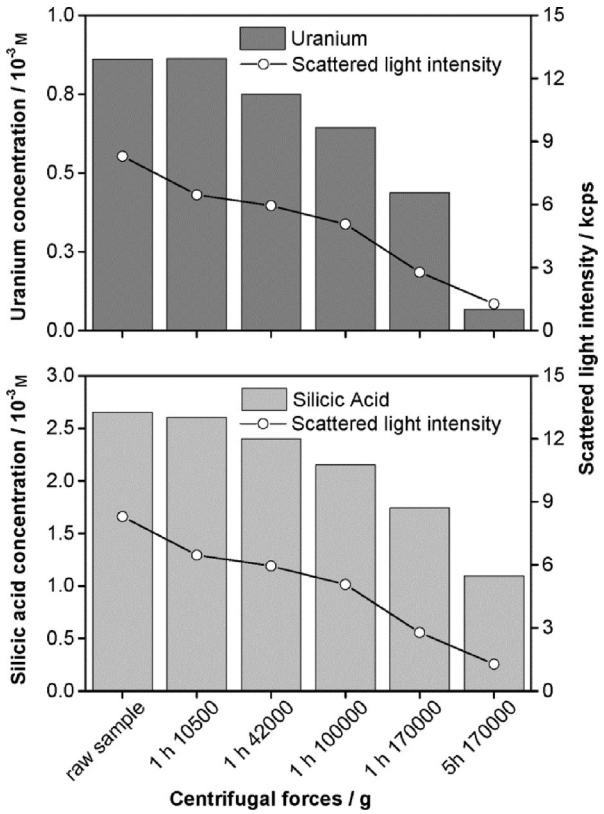

Figure 3. Uranium concentration, silicic acid concentration, and scattered light intensity of a colloidal suspension of U^{IV} oxyhydroxy silicate colloids after ultracentrifugation with different acceleration. Initial concentrations: $U^{IV}=8.6\times10^{-4}$ M, $Si^{IV}=2.7\times10^{-3}$ M, $CO_3^{2-}=5\times10^{-2}$ M, pH 7.8. The particles consist of U^{IV} and silica. Diameter of the particles: < 20 nm. Reproduced with permission from Ref. [51]. Copyright 2010, Elsevier Ltd.

© 2016 The Authors. Published by Wiley-VCH Verlag GmbH & Co. KGaA, Weinheim

effect) for a suspension of U^{IV} oxyhydroxy silicate colloids after centrifugation at different centrifugal accelerations. A weak centrifugation does not influence the concentrations. However, the larger the centrifugal force is, the stronger removal of U from the solution results, indicating that almost all the U is in a colloid-borne form. This is accompanied by a parallel removal of a silica fraction which demonstrates that the colloids consist of U and Si. From the centrifugal acceleration required for removal, it can be deduced that the prevailing size of the colloids is less than 20 nm (see Table 2 in Ref. [51]). Figure 4 shows the results of an alternative experiment on the samples obtained from the ultrafiltration process. The filtration with $\geq$300 kDa does not decrease the U and Si concentrations in the filtrates. However, the U and Si concentrations are decreased by filtration with smaller pore sizes. With a pore size of $\leq$10 kDa, uranium virtually disappears from the solution, indicating that almost all the U occurs in a colloid-borne form. A significant fraction of the silicic acid is removed by the smaller filter pores as well. It should be noted, however, that the silicic acid was not filterable without the addition of An^{IV}. Particle sizes of the U^{IV} oxyhydroxy silicate colloids can be estimated to be around 3 to 20 nm from Figure 4 (see Table 1 of Ref. [51]). In Figure 5 the results of photon correlation spectroscopy on a suspension of Np^{IV} oxyhydroxy silicate colloids are given. A particle size of the same order of magnitude as in Figure 3 and 4 is found. If the silicic acid concentration is sufficiently high, ultracentrifugation, ultrafiltration, and photon correlation spectroscopy all indicate a particle size of $<$20 nm for all investigated An^{IV} oxyhydroxy silicate colloids.

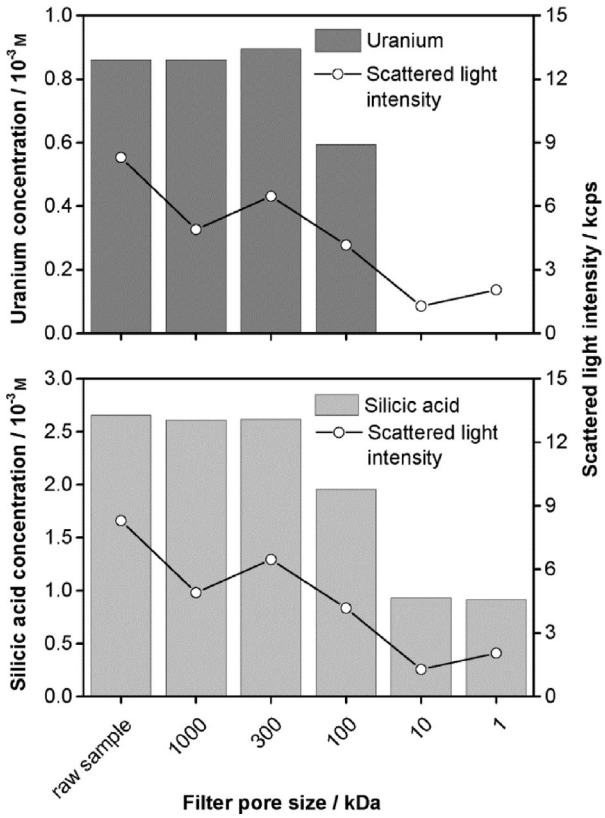

Figure 4. Uranium concentration, silicic acid concentration, and scattered light intensity of a colloidal suspension of U^{IV} oxyhydroxy silicate colloids after ultrafiltration with different filter pore sizes. Initial concentrations: $U^{IV}=8.6\times10^{-4}$ M, $Si^{IV}=2.7\times10^{-3}$ M, $CO_3^{2-}=5\times10^{-2}$ M, pH 7.8. The particles consist of U^{IV} and silica. Diameter of the particles: 3-20 nm. Reproduced with permission from Ref. [51]. Copyright 2010, Elsevier Ltd.

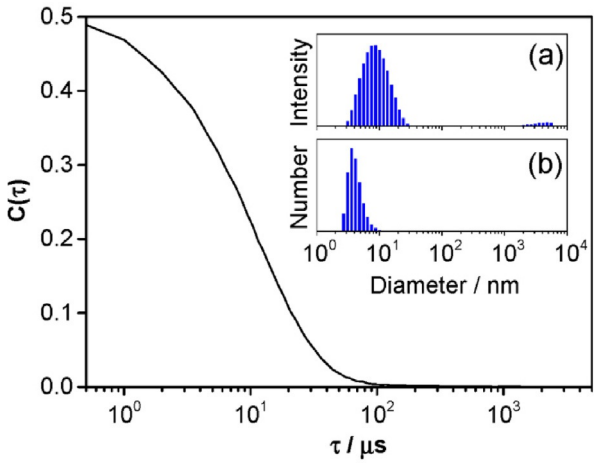

Figure 5. Autocorrelation function and particle size distribution of Np^{IV} oxyhydroxy silicate colloids. $Np^{IV}=10^{-3}$ M, $Si^{IV}=3.0\times10^{-3}$ M, $CO_3^{2-}=10^{-1}$ M. a) Light-intensity weighted particle size distribution. b) Number weighted particle size distribution. The vast majority of the particles has a size of 5 to 10 nm. Reproduced with permission from Ref. [67]. Copyright 2015, Royal Society of Chemistry.

3.2. Long-Term Stability

Figure 6 shows the scattered light intensities of suspensions of U^{IV} and Th^{IV} oxyhydroxy silicate colloids. Since the scattered light intensity depends on the optical experiment setup in light scattering experiments of this type, these values are given in comparison with a reference value, that is, the scattered light intensity of the solvent (pure water). The figure

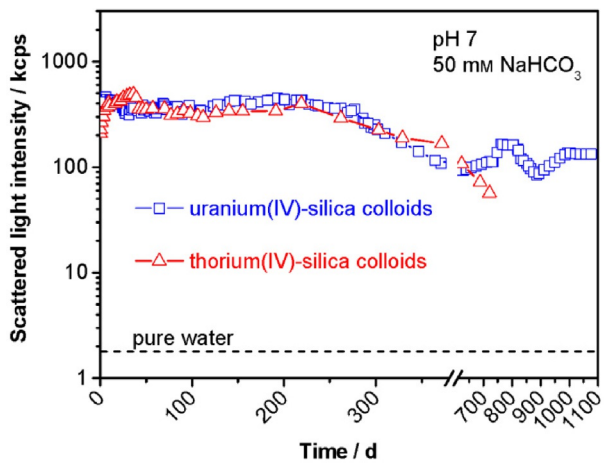

Figure 6. Time variation of scattered light intensity from solutions containing waterborne U^{IV} oxyhydroxy silicate (blue) and Th^{IV} oxyhydroxy silicate (red) nanoparticles ($U^{IV}=9\times10^{-4}$ M, $Th^{IV}=8\times10^{-4}$ M). The scattered light intensities are compared with that of pure water. The colloids are stable over years.[51,52] Reproduced with permission from Refs. [51] and [52]. Copyrights 2010 and 2012, Elsevier Ltd.

© 2016 The Authors. Published by Wiley-VCH Verlag GmbH & Co. KGaA, Weinheim

demonstrates that An^{IV} oxyhydroxy silicate colloids of a concentration of about 10^{-3} M can be stabilized in the waterborne state over years. An^{IV} oxyhydroxide colloids, on the other hand, would greatly precipitate within a few hours at a concentration of 10^{-3} M and a pH of 7. Stable An^{IV} oxyhydroxide colloids can only be obtained at concentrations of about 10^{-6} M (see Figure 2).

In Figure 6, we see the time variation of scattered light intensity from solutions containing waterborne U^{IV} oxyhydroxy silicate (blue) and Th^{IV} oxyhydroxy silicate (red) nanoparticles ($U^{IV} = 9\times10^{-4}$ M, Th(IV) $= 8\times10^{-4}$ M). The scattered light intensities are compared with that of pure water. The colloids are stable over years.[51,52]

3.3. Zeta Potential

In Figure 7 zeta potential vs. pH curves for silica-free Th^{IV} oxyhydroxide colloids, Th^{IV} oxyhydroxy silicate colloids, and pure SiO_2 colloids are depicted (laser Doppler velocimetry). It shows that the presence of silica shifts the curve for Th^{IV} oxyhydroxide toward that for pure SiO_2. This moves the IEP of the Th^{IV} colloids to lower pH values, that is, the particles become negatively charged in the near-neutral/slightly-alkaline region, and they tend to repel each other stronger (e.g., at pH 8 in Figure 7). The latter is one of the reasons for the stabilization of the An^{IV} colloids by silicic acid at An^{IV} concentrations much higher than observed for the silica-free An^{IV} oxyhydroxide colloids. The second reason for the high stability is that non-DLVO forces increasingly play a role with the admixture of silica (see below). A similar shift of the zeta potential toward more negative values and the IEP toward lower pH values by the admixture of silica is also observed for U^{IV} colloids.[51]

3.4. Internal Structure

The structure of An^{IV} oxyhydroxy silicate colloids has been investigated by extended X-ray absorption fine structure (EXAFS)

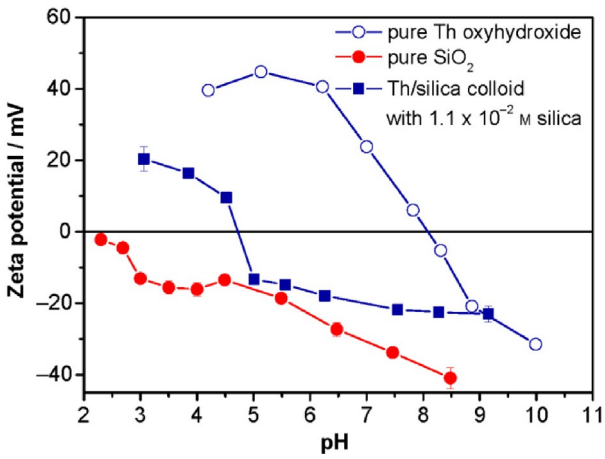

Figure 7. Variation of Zeta potentials of Th^{IV} oxyhydroxide, SiO_2, and Th^{IV} oxyhydroxy silicate colloids as a function of pH. $Th^{IV} = 10^{-3}$ M; initial carbonate $= 5\times10^{-2}$ M. The curve for the Th^{IV} oxyhydroxide is shifted toward that of pure silica when silica is added in the system (i.e. Th^{IV}/silica colloids). Reproduced with permission from Ref. [52]. Copyright 2012, Elsevier Ltd.

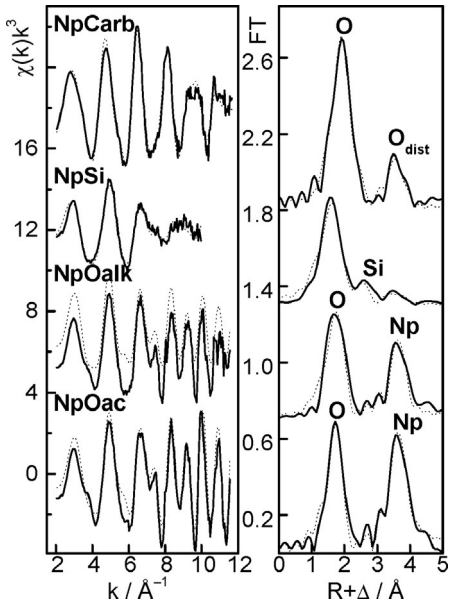

Figure 8. Np L_3 edge EXAFS spectra (left, k^3-weighted) and their corresponding Fourier transforms (right) of an aqueous solution of 9 mM Np^{IV} in 1 M $NaHCO_3$ (NpCarb), a colloidal solution of 1 mM Np^{IV} and 3 mM Si in 0.1 M $NaHCO_3$ (NpSi), Np^{IV} precipitate obtained by diluting a slightly basic Np^{IV} solution with water (NpOalk), and Np^{IV} precipitate obtained by neutralizing Np^{IV} in HNO_3 with NaOH (NpOac). Reproduced with permission from Refs.[44] and [67]. Copyrights 2015, Royal Society of Chemistry.

spectroscopy, high-energy X-ray scattering (HEXS), X-ray photoelectron spectroscopy (XPS), neutron scattering, high-resolution transmission electron microscopy (HR-TEM), and ^{29}Si solid state NMR.[51,52,67] Figure 8 shows EXAFS spectra for Np^{IV}-silica colloids and several Np(IV) reference systems as well as their Fourier transforms. The fit parameters derived from the EXAFS spectra (atomic distances, coordination numbers) are given in Refs. [44] and [67]. The results indicate a relatively short Th–Si distance of ~3.11 Å. This distance is characteristic of the silica coordination with a bidentate mode (or the edge-sharing coordination in the terminology of coordination polyhedra), while the monodentate coordination (e.g., simple adsorption of Np^{IV} onto solid silica) results in a significantly longer Th–Si distance. The EXAFS results show that Np–O–Np bonds in the Np(IV) oxyhydroxide colloids are partly replaced with Np–O–Si bonds due to incorporation of silica into the structure, as shown in Figure 9, finally forming $[(Np,Si)O_n(OH)_{4-n}\cdot xH_2O]^{4-2n-(4-n)}$. This replacement with Np–O–Si bonds accounts for the short Th–Si distance. Structural inclusion of the silica was also observed for U^{IV} and Th^{IV} oxyhydroxy silicate colloids.[51,52] It had, furthermore, been derived from X-ray diffraction results for the An^{IV}-analogue Zr^{IV}.[62] For all these colloids, the incorporation of silica results in a structure which has a near-order similar to that of the silicate mineral coffinite ($USiO_4$), even if the colloids are much more amorphous than coffinite. The disordered structure of the colloids also supresses significantly the intensity of the Np–Np peak of the EXAFS-FT in Figure 8 which is due to destructive interference effects caused by different Np–Np distances. This phenomenon is described in more detail in Ref. [52].

© 2016 The Authors. Published by Wiley-VCH Verlag GmbH & Co. KGaA, Weinheim

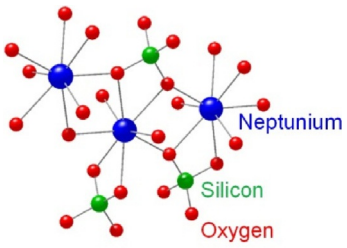

Figure 9. Structure of neptunium(IV) oxyhydroxy silicate colloids derived from EXAFS. Reproduced with permission from Ref. [67]. Copyright 2015, Royal Society of Chemistry.

The EXAFS results are complementary to the results from the other methods, in particular HEXS and NMR.[52] Figure 10 shows the NMR spectra of Th^{IV} oxyhydroxy silica colloids as a function of Si/Th ratio. The chemical shift δ_{29Si} is a good indicator to investigate how many oxygen atoms in the $[SiO_4]$ tetrahedron are shared with other silica units. The peak Q^0, indicating a monomeric silicate anion, appears at the less negative side of the spectrum and shows almost constant shifts of 10 ppm toward the more negative side for each added Si–O–Si bond if the Si/Th ratio of the colloids increases. Huttonite, β-$ThSiO_4$, was used as a reference of δ_{29Si} in the Th^{IV} oxyhydroxy silicate colloids. The structure of huttonite represents a typical orthosilicate in which SiO_4 units do not share oxygen atoms with other SiO_4 tetrahedra. The ^{29}Si NMR spectrum shows a chemical shift δ_{29Si} of −82.4 ppm. The peaks observed for the Th^{IV} silicate colloid particles exhibit a significant broadening and overlapping of different Si–O contributions. This is in line with the EXAFS results indicating that the colloids are disordered structures and the oxygens in the structure have a variety of different coordination geometry. The position of the main peak of the sample "Si/Th = 0.32" is comparable with the Q^0 peak of β-$ThSiO_4$, indicating that the silicates in this sample are in the isolated orthosilicate form. The silicic acid concentration in the relevant aqueous sample was 0.95 mM, which is well below the "mononuclear wall". Colloids with higher Si/Th ratios (i.e., the silicic acid concentrations above the "mononuclear wall") show an increase of Si–O–Si bonds in the structure, which is indicated by more negative chemical shifts. When the silica is in excess, represented by the sample "Si/Th = 5.84", the structure is mainly dominated by Q^3 units at −98 ppm with additional contributions of Q^2 at −88.6 ppm and Q^4 at −109.8 ppm, suggesting the progress of silica polymerization. The formation of polynuclear silica species can already occur in the solution when the silica concentration is above the "mononuclear wall" of 2×10^{-3} M.

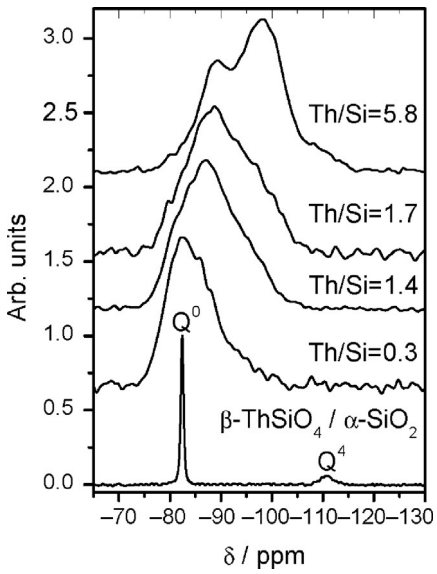

Figure 10. ^{29}Si cross polarization magic angle spinning (CP/MAS) and single-pulse MAS spectra of Th^{IV} silicate solutions with different Si/Th ratios and reference compounds of β–$ThSiO_4$ and α–SiO_2, $\nu_R = 5$ kHz. Reproduced with permission from Ref. [52]. Copyright 2012, Elsevier Ltd.

XPS measurements provided further information on the composition of Th^{IV} oxyhxdroxy silicate colloids.[52] The results showed that the chemical composition of the colloids is homogeneous as long as the silicic acid concentration is below the "mononuclear wall". When the silicic acid concentration exceeds the "mononuclear wall" level, silica starts being enriched on the colloid surfaces, finally forming a silica-rich layer on the surface. UV/Vis spectroscopy can also provide qualitative information about the formation of An^{IV} colloids. This has been demonstrated, for instance, for Np^{IV} oxyhydroxy silicate colloids which can be detected by the characteristic "colloid peak" at 740–746 nm.[67]

The structure of An^{IV} oxyhydroxy silicate colloids is strongly influenced by their formation process. In the hitherto reported experiments (Refs. [51, 52, and 67]), the initial step of the colloid formation was the hydrolysis of dissolved An^{IV} carbonate complexes. The resultant An^{IV} hydrolysis products further react either with other An^{IV} hydroxide species or with silicic acid to induce further hydrolysis and/or polymerization. If the initial silicic acid solution is below the "mononuclear wall", silica is incorporated into the An–O framework of the colloid structure as isolated monomers. On the other hand, when the initial silicic acid concentration exceeds the "mononuclear wall", silica units are polymerized with one another which results in the formation of polysilicic acid species in the initial solution, such as $Si_2O_3(OH)_4^{2-}$, $Si_3O_5(OH)_5^{3-}$, $Si_4O_8(OH)_4^{4-}$ or other oligomers with low molecular weights, and in the incorporation into the colloids as such oligomers. The enrichment of silica on the colloid particle surface is probably controlled by the kinetics of colloid formation. That is, An^{IV} contributes to a fast reaction kinetics which induces polymerization within the first several minutes of reaction. When the An^{IV} concentration in the sample solution is decreased, the overall reaction kinetics become slower and are controlled by the polymerization of silicic acid and oligomeric silica species. When further approaching to the steady state, the reaction kinetics is primarily dominated by silica polymerization on the particle surface.[52]

3.5. Colloid Stabilization Mechanisms

The classical approach to describe the stability of colloids is the application of the DLVO theory developed by Derjaguin, Landau, Verwey, and Overbeek. This theory is based on the su-

© 2016 The Authors. Published by Wiley-VCH Verlag GmbH & Co. KGaA, Weinheim

perposition of repulsive electrostatic double layer forces and the attractive Van der Waals force.[72–74] Many colloidal systems obey the DLVO theory but there are also many other systems which do not follow this theory. The latter applies in particular to very hydrophobic or very hydrophilic colloids.[75] In these cases, "structural forces", which are caused, for instance, by the water molecules around the particles, could play an important role. Such forces can be attributed to hydrogen bonding,[73,76,77] hydrophobic interactions,[73,78] steric interactions[73,74] etc. For oxide colloids, Koopal[79] suggested to distinguish between

i) colloids with gibbsite-type surfaces and
ii) colloids with silica-type surfaces.

The gibbsite-type colloids, which include colloids of An^{IV} dioxides and their analogs, for example ZrO_2 and TiO_2, are amphoteric and exhibit the typical "charge vs. pH" curves showing a point of zero charge in the middle of the pH scale. This type of colloids follows the classical DLVO theory quite well when the electrolyte concentration is relatively low. The silica-based colloids, on the other hand, show a more complex behavior which is due to several special properties of silica such as its low Hamaker constant, its strong tendency to form hydrogen bonds and its high hydrophilicity.[70] Silica colloids are typically acidic and can only carry negative charges, according to Koopal. Other studies reported IEPs for silica of pH 1.5 to 3.[49,70, 80,81] Silica-based colloids are more stable than gibbsite-type colloids and, hence, deviate significantly from the behavior expected from the DLVO theory.[82] They show a stability *maximum* at the IEP which contradicts the DLVO model sharply.[76,80,82] A stability *minimum* is found at pH 4 to 7, that is far from the IEP.[76] Furthermore, there is an influence of the particle size; silica nanoparticles of $\geq$50 nm obey the DLVO model better than the very small ones.[74,83] A variety of models have been developed to explain the complex non-DLVO systems including the silica colloids, namely the *hydration force model for silica*,[76,77,80,82–86] the *gel layer model*,[87–89] the *hairy layer mode*,[74,90–92] or the *roughness model*.[93] However, there is only a limited number of studies dealing with the binary systems containing both metal oxide and silica (ZrO_2/silica,[94] ferrihydrite/silica,[65] UO_2/silica,[51] ThO_2/silica[52]).

In the case of metal oxyhydroxides and silica, protons (H^+) and/or hydroxide ions (OH^-) are the potential-determining ions which control the surface charge of colloids, (i.e., zeta potential).[81,95] Figure 7 demonstrates that the addition of silica to the colloidal solution of Th^{IV} oxyhydroxide drastically changes the shape of the "zeta potential vs. pH" curve. That is, the pH curve is shifted toward the curve of pure silica colloids. Similar results were obtained by Dyer et al. for binary silica-ferrihydrite colloids.[65] From their zeta potential vs. pH curves, Dyer et al. concluded that the surfaces of the particles are a "mixture" of ferrihydrite and silica. We can expect the same situation on the surfaces of the Th^{IV} oxyhydroxy silicate particles, reflecting the behavior of both Th^{IV} oxyhydroxide and silica. The negative charge of the colloids observed in the case of silica addition to the Th^{IV} oxyhydroxide can contribute to the repelling force that stabilizes the particles in near-neutral solutions.

However, the formation of the binary Th^{IV} oxyhydroxy silicate may also reflect a transition from metal-oxide-type colloids (or, according to the Koopal's terminology, "gibbsite-type" colloids) to silica-type colloids (types i and ii). Even though the electrostatic repulsion plays an important role in the stability of these colloidal particles, particularly in the near-neutral pH region, non-DLVO forces could also be of importance. The non-DLVO forces could explain the reason why the negatively charged Th^{IV} oxyhydroxy silicate colloids are more stable at a pH around 7 than the positively charged Th^{IV} oxyhydroxide colloids (Figure 7), despite the fact that the absolute zeta potential values of these colloids are well comparable. Further studies are required to quantify the DLVO- and non-DLVO contributions to the stabilization of An^{IV}-silica colloids.

4. Concluding Remarks and Future Outlook

This review demonstrates that the formation of the coffinite-like An^{IV} oxyhydroxy silicate colloids can result in concentrations of waterborne An^{IV} colloids which are higher than the "equilibrium concentrations"[53] of An^{IV} oxyhydroxide colloids by a factor of at least 10^3 at near-neutral pH (see Figures 2, 3, and 4). Despite this fact, as mentioned above, previous An^{IV} colloid research has strongly been focused on An^{IV} oxyhydroxide colloids. An^{IV} oxyhydroxy silicate colloids may not have been as attractive as the An^{IV} oxyhydroxide colloids for the coordination chemist and the microscopist because they are poorly structured (i.e., amorphous) which might make them less attractive from the experimental point of view. However, in terms of geochemistry and environmental science, An^{IV} oxyhydroxy silicate colloids could be of high importance.

There is only a limited number of studies discussing the potential generation of An^{IV} colloids in the real aquatic environment. Kalmykov et al. reported the formation of U^{IV} oxyhydroxide colloids in anoxic groundwaters at the Mayak Site (Russia).[96] Kozai et al. searched for the formation of silica-containing U colloids in the silica-rich anoxic saline groundwater at the Horonobe underground research laboratory (Japan).[97] By means of size-exclusion chromatography, these authors found out that U^{IV} was bound neither to clay or zeolite particles nor to the organic colloids present in the near-neutral groundwater, but it was associated with neutral silica species which were monomeric silicic acid or low molecular weight polymeric silicic species of less than 1.5 kDa. The uranium concentration of the Horonobe groundwater is only 10^{-10} M. It seems that An^{IV} species form truly dissolved neutral silicate complexes in solutions containing silicic acid if the actinide concentration is very low, but that colloids are produced if the An^{IV} concentration is in the range of 10^{-3} M as in the previous laboratory experiments on An^{IV} oxyhydroxy silicate colloids[51,52,67] and as to be expected in the near-field of a nuclear waste repository after the access of water.

In the scenario of the potential leakage of radioactive contaminants from a nuclear waste repository into the near-field environment, the generation of oxyhydroxy silicate type colloids cannot be ruled out as silicic acid is ubiquitous in groundwater. Additionally, there are other sources of silicic

 © 2016 The Authors. Published by Wiley-VCH Verlag GmbH & Co. KGaA, Weinheim

acid in the waste repository, such as vitrification materials, cement, bentonite, or injected grout silica, regardless of the design of waste repositories (see Ref. [12] and references therein). Thus, An^{IV} oxyhydroxy silicate colloids may be able to stabilize significant amounts of An^{IV} in a waterborne form. Serious concern could arise if An^{IV} could readily diffuse through the bentonite barrier of a nuclear waste repository via the formation of silica-containing An^{IV} nanoparticles. As a matter of fact, organic macromolecules of a similar size (30 kDa) could pass through the compacted bentonite barrier under certain conditions.[98] Another concern would be the behavior of An^{IV} oxyhydroxy silicate nanoparticles when bentonite pore waters containing such particles are diluted in the pore water–freshwater mixing zone[99] or via the intrusion of glacial meltwater produced after a possible future ice age.[100] Such dilution processes would decrease the ionic strength, eventually stabilizing colloids.

U^{IV} oxyhydroxy silicate colloids might also play an important role in the formation of ore deposits. In 1962, Moench hypothesized that the generation of uranium colloids is crucial for the paragenesis of coffinitic uranium ore deposits.[101] U^{IV} oxyhydroxy silicate colloids form a candidate class of colloids accomplishing the colloid-chemical processes necessary for the formation of coffinitic uranium ore. Furthermore, An^{IV} oxyhydroxide colloids may also be involved in the "coffinitization" of UO_2-based spent fuel, a phenomenon expected in nuclear waste repositories after the access of water[102–109] which occurs via the dissolution and the reprecipitation of An^{IV}[110,111] and which is of significance for the behavior of spent fuel.

An^{IV} oxyhydroxides form colloids which are often stabilized in the waterborne state by repulsive electrostatic double-layer forces in solutions of low to moderate electrolyte concentrations. In the case of An^{IV} oxyhydroxy silicate colloids, the picture is more complex. For such colloids, non-DLVO forces attributable to hydrogen bonding, steric effects, etc. increasingly play a role in addition to the electrostatic forces with increasing silica content of the colloids. At high silica content, the behavior of the particles resembles more that of pure silica particles than that of An^{IV} oxhydroxide particles. This results in an increase of colloid stability (silica nanoparticles are known for their high colloidal stability). The properties and the behavior of An^{IV} oxyhydroxy silicate colloids and the reasons for their high colloidal stability need to be investigated in greater detail.

Keywords: actinides · colloids · environmental chemistry · silicates · spectroscopic methods

[1] *Guidelines for Drinking-water Quality, 4th ed.* (NLM classification: WA 675), WHO, Geneva, **2011**.
[2] *Uranium in Drinking-water, Background Document for Development of WHO Guidelines for Drinking-water Quality*, WHO/SDE/WSH/03.04/118/Rev/1, **2011**.
[3] B. D. Honeyman, *Nature* **1999**, *397*, 23–24.
[4] A. B. Kersting, D. W. Efurd, D. L. Finnegan, D. J. Rokop, D. K. Smith, J. L. Thompson, *Nature* **1999**, *397*, 56–59.
[5] A. P. Novikov, S. N. Kalmykov, S. Utsunomiya, R. C. Ewing, F. Horreard, A. Merkulov, S. B. Clark, V. V. Tkachev, B. F. Myasoedov, *Science* **2006**, *314*, 638–641.
[6] P. C. Burns, R. C. Ewing, A. Navrotsky, *Science* **2012**, *335*, 1184–1188.
[7] C. Walther, M. A. Denecke, *Chem. Rev.* **2013**, *113*, 995–1015.
[8] K. Maher, J. R. Bargar, G. E. Brown Jr., *Inorg. Chem.* **2013**, *52*, 3510–3532.
[9] A. B. Kersting, *Inorg. Chem.* **2013**, *52*, 3533–3546.
[10] B. Grambow, *Elements* **2006**, *2*, 357–364.
[11] M. Altmaier, X. Gaona, T. Fanghänel, *Chem. Rev.* **2013**, *113*, 901–943.
[12] H. Zänker, C. Hennig, *J. Contam. Hydrol.* **2014**, *157*, 87–105.
[13] V. Neck, J. I. Kim, *Radiochim. Acta* **2001**, *89*, 1–16.
[14] V. Neck, J. I. Kim, B. S. Seidel, C. M. Marquardt, K. Dardenne, M. P. Jensen, W. A. Hauser, *Radiochim. Acta* **2001**, *89*, 439–446.
[15] C. Bitea, R. Muller, V. Neck, C. Walther, J. I. Kim, *Colloids Surf. A* **2003**, *217*, 63–70.
[16] C. Walther, H. R. Cho, C. M. Marquardt, V. Neck, A. Seibert, J. I. Yun, T. Fanghänel, *Radiochim. Acta* **2007**, *95*, 7–16.
[17] V. Neck, R. Müller, M. Bouby, M. Altmaier, J. Rothe, M. Denecke, J. I. Kim, *Radiochim. Acta* **2002**, *90*, 485–494.
[18] D. Rai, A. R. Felmy, S. M. Sterner, D. A. Moore, M. J. Mason, C. F. Novak, *Radiochim. Acta* **1997**, *79*, 239–247.
[19] D. Rai, A. R. Felmy, D. A. Moore, M. J. Mason, *Mater. Res. Soc. Symp. Proc.* **1994**, *353*, 1143–1150.
[20] D. Rai, N. J. Hess, A. R. Felmy, D. A. Moore, M. Yui, *Radiochim. Acta* **1999**, *84*, 159–169.
[21] D. Rai, D. A. Moore, C. S. Oakes, M. Yui, *Radiochim. Acta* **2000**, *88*, 297–306.
[22] J. L. Ryan, D. Rai, *Inorg. Chem.* **1987**, *26*, 4140–4142.
[23] T. Bundschuh, R. Knopp, R. Müller, J. I. Kim, V. Neck, T. Fanghänel, *Radiochim. Acta* **2000**, *88*, 625–629.
[24] R. Knopp, V. Neck, J. I. Kim, *Radiochim. Acta* **1999**, *86*, 101–108.
[25] P. Thiyagarajan, H. Diamond, L. Soderholm, É. P. Horwitz, L. M. Toth, L. K. Felker, *Inorg. Chem.* **1990**, *29*, 1902–1907.
[26] R. E. Wilson, S. Skanthakumar, G. Sigmon, P. C. Burns, L. Soderholm, *Inorg. Chem.* **2007**, *46*, 2368–2372.
[27] L. Soderholm, P. M. Almond, S. Skanthakumar, R. E. Wilson, P. C. Burns, *Angew. Chem. Int. Ed.* **2008**, *47*, 298–302; *Angew. Chem.* **2008**, *120*, 304–308.
[28] C. Walther, M. Fuss, S. Buchner, *Radiochim. Acta* **2008**, *96*, 411–425.
[29] C. Walther, J. Rothe, B. Brendebach, M. Fuss, M. Altmaier, C. M. Marquardt, S. Büchner, H.-R. Cho, J.-I. Yun, *Radiochim. Acta* **2009**, *97*, 199–207.
[30] R. E. Wilson, S. Skanthakumar, L. Soderholm, *Angew. Chem. Int. Ed.* **2011**, *50*, 11234–11237; *Angew. Chem.* **2011**, *123*, 11430–11433.
[31] K. E. Knope, L. Soderholm, *Chem. Rev.* **2013**, *113*, 944–994.
[32] S. Takao, K. Takao, W. Kraus, F. Ernmerling, A. C. Scheinost, G. Bernhard, C. Hennig, *Eur. J. Inorg. Chem.* **2009**, 4771–4775.
[33] K. E. Knope, R. E. Wilson, M. Vasiliu, D. A. Dixon, L. Soderholm, *Inorg. Chem.* **2011**, *50*, 9696–9704.
[34] C. Hennig, S. Takao, K. Takao, S. Weiss, W. Kraus, F. Emmerling, A. C. Scheinost, *Dalton Trans.* **2012**, *41*, 12818–12823.
[35] K. Takao, S. Takao, A. C. Scheinost, G. Bernhard, C. Hennig, *Inorg. Chem.* **2012**, *51*, 1336–1344.
[36] M. Vasiliu, K. E. Knope, L. Soderholm, D. A. Dixon, *J. Phys. Chem. A* **2012**, *116*, 6917–6926.
[37] J. Qiu, P. C. Burns, *Chem. Rev.* **2013**, *113*, 1097–1120.
[38] S. Dahou, C. Hennig, P. Moisy, S. Petit, A. C. Scheinost, G. Subra, C. Vidaud, C. Den Auwer, *Radiochim. Acta* **2013**, *101*, 367–372.
[39] Y. J. Hu, K. E. Knope, S. Skanthakumar, L. Soderholm, *Eur. J. Inorg. Chem.* **2013**, 4159–4163.
[40] G. Rousseau, M. Fattahi, B. Grambow, L. Desgranges, F. Boucher, G. Ouvrard, N. Millot, J. C. Niepce, *J. Solid State Chem.* **2009**, *182*, 2591–2597.
[41] D. J. Dzimitrowicz, P. J. Wiseman, D. Cherns, *J. Colloid Interface Sci.* **1984**, *103*, 170–177.
[42] B. A. Powell, Z. R. Dai, M. Zavarin, P. H. Zhao, A. B. Kersting, *Environ. Sci. Technol.* **2011**, *45*, 2698–2703.
[43] A. Y. Romanchuk, S. N. Kalmykov, A. V. Egorov, Y. V. Zubavichus, A. A. Shiryaev, O. N. Batuk, S. D. Conradson, D. A. Pankratov, I. A. Presnyakov, *Geochim. Cosmochim. Acta* **2013**, *121*, 29–40.

© 2016 The Authors. Published by Wiley-VCH Verlag GmbH & Co. KGaA, Weinheim

[44] R. Husar, R. Hübner, C. Hennig, P. M. Martin, M. Chollet, S. Weiss, T. Stumpf, H. Zänker, A. Ikeda-Ohno, *Chem. Commun.* **2015**, *51*, 1301 – 1304.
[45] F. Takasaki, K. Fujiwara, Y. Nakajima, T. Nishikawa, N. Ogawa, *Chem. Lett.* **2014**, *43*, 196 – 198.
[46] A. Ikeda-Ohno, C. Hennig, S. Weiss, T. Yaita, G. Bernhard, *Chem. Eur. J.* **2013**, *19*, 7348 – 7360.
[47] I. R. Triay, D. E. Hobart, A. J. Mitchell, T. W. Newton, M. O. Ott, P. D. Palmer, R. S. Rundberg, J. L. Thompson, *Radiochim. Acta* **1991**, *52 – 53*, 127 – 132.
[48] A. Ikeda-Ohno, C. Hennig, S. Tsushima, A. C. Scheinost, G. Bernhard, T. Yaita, *Inorg. Chem.* **2009**, *48*, 7201 – 7210.
[49] G. A. Parks, *Chem. Rev.* **1965**, *65*, 177 – 198.
[50] A. I. Abdel-Fattah, D. Zhou, H. Boukhalfa, S. Tarimala, S. D. Ware, A. A. Keller, *Environ. Sci. Technol.* **2013**, *47*, 5626 – 5634.
[51] I. Dreissig, S. Weiss, C. Hennig, G. Bernhard, H. Zänker, *Geochim. Cosmochim. Acta* **2011**, *75*, 352 – 367.
[52] C. Hennig, S. Weiss, D. Banerjee, E. Brendler, V. Honkimäki, G. Cuello, A. Ikeda-Ohno, A. C. Scheinost, H. Zänker, *Geochim. Cosmochim. Acta* **2013**, *103*, 197 – 212.
[53] M. Altmaier, V. Neck, T. Fanghänel, *Radiochim. Acta* **2004**, *92*, 537 – 543.
[54] J. Rothe, C. Walther, M. A. Denecke, T. Fanghanel, *Inorg. Chem.* **2004**, *43*, 4708 – 4718.
[55] D. Langmuir, *Geochim. Cosmochim. Acta* **1978**, *42*, 547 – 569.
[56] J. I. Kim, C. Walther in *Environmental Colloids and Particles, Series: IUPAC Series on Analytical and Physical Chemistry of Environmental Systems* (Eds.: K. J. Wilkinson, J. R. Lead), John Wiley & Sons, **2007**, pp. 555 – 612.
[57] P. C. Burns, K. A. Kubatko, G. Sigmon, B. J. Fryer, J. E. Gagnon, M. R. Antonio, L. Soderholm, *Angew. Chem. Int. Ed.* **2005**, *44*, 2135 – 2139; *Angew. Chem.* **2005**, *117*, 2173 – 2177.
[58] P. B. Duval, C. J. Burns, D. L. Clark, D. E. Morris, B. L. Scott, J. D. Thompson, E. L. Werkema, L. Jia, R. A. Andersen, *Angew. Chem. Int. Ed.* **2001**, *40*, 3357 – 3361; *Angew. Chem.* **2001**, *113*, 3461 – 3465.
[59] G. Marcu, M. Rusu, D. Rusu, *J. Radioanal. Nucl. Chem.* **1999**, *242*, 119 – 122.
[60] S. V. Krivovichev, V. Kahlenberg, R. Kaindl, E. Mersdorf, I. G. Tananaev, B. F. Myasoedov, *Angew. Chem. Int. Ed.* **2005**, *44*, 1134 – 1136; *Angew. Chem.* **2005**, *117*, 1158 – 1160.
[61] R. Siever in *Silicon-abundunce in Natural Waters, Handbook of Geochemistry* (Eds.: K. H. Wedepohl), Springer, Berlin, Heidelberg, New York, **1972**, pp. 14-I-1 – 14-I-6.
[62] A. Adamski, P. Jakubus, Z. Sojka in *Doped Nanopowders: Synthesis, Characterisation Applications. Book Series: Solid State Phenomena* (Eds. W. Lojkowski, J. R. Blizzard, U. Narkiewicz, J. D. Fidelus), Trans Tech Publications, Päffikon, Switzerland **2007**, *128*, 89 – 96.
[63] M. G. Browman, R. B. Robinson, G. D. Reed, *Environ. Sci. Technol.* **1989**, *23*, 566 – 572.
[64] R. B. Robinson, G. D. Reed, B. Frazier, *J. Am. Water Works Assoc.* **1992**, *84*, 77 – 82.
[65] L. Dyer, P. D. Fawell, O. M. G. Newman, W. R. Richmond, *J. Colloid Interface Sci.* **2010**, *348*, 65 – 70.
[66] P. A. Panak, M. A. Kim, R. Klenze, J. I. Kim, T. Fanghänel, *Radiochim. Acta* **2005**, *93*, 133 – 139.
[67] R. Husar, S. Weiss, C. Hennig, R. Hübner, H. Zänker, *Environ. Sci. Technol.* **2015**, *49*, 665 – 671.
[68] W. Stumm, H. Huper, L. Champlin, *Environ. Sci. Technol.* **1967**, *1*, 221 – 227.
[69] P. D. Taylor, R. Jugdaohsingh, J. J. Powell, *J. Am. Chem. Soc.* **1997**, *119*, 8852 – 8856.
[70] R. K. Iler, *The Chemistry of Silica*, John Wiley & Sons, Inc., New York, **1979**.
[71] H. Zänker, G. Hüttig, T. Arnold, H. Nitsche, *Aquat. Geochem.* **2006**, *12*, 299 – 325.
[72] J. Eastman in *Colloid Science. Principles, methods and applications* (Ed. T. Cosgrove). Blackwell Publishing, Oxford, **2005**, pp. 36 – 49.
[73] D. Grasso, K. Subramaniam, M. Butkus, K. Strevett, *Re/Views Environ. Sci. Bio/Technol.* **2002**, *1*, 17 – 38.
[74] M. Kobayashi, F. Juillerat, P. Galletto, P. Bowen, M. Borkovec, *Langmuir* **2005**, *21*, 5761 – 5769.
[75] H. Yotsumoto, R. H. Yoon, *J. Colloid Interface Sci.* **1993**, *157*, 426 – 433.
[76] J.-P. Chapel, *Langmuir* **1994**, *10*, 4237 – 4243.
[77] A. Grabbe, R. G. Horn, *J. Colloid Interface Sci.* **1993**, *157*, 375 – 383.
[78] J. N. Israelachvili, R. M. Pashley, *J. Colloid Interface Sci.* **1984**, *98*, 500 – 514.
[79] L. K. Koopal, *Electrochim. Acta* **1996**, *41*, 2293 – 2305.
[80] L. H. Allen, E. Matijevic, *J. Colloid Interface Sci.* **1969**, *31*, 287 – 296.
[81] J. Sonnefeld, M. Löbbus, W. Vogelsberger, *Colloids Surf. A* **2001**, *195*, 215 – 225.
[82] H. Yotsumoto, R. H. Yoon, *J. Colloid Interface Sci.* **1993**, *157*, 434 – 441.
[83] R. D. Harding, *J. Colloid Interface Sci.* **1971**, *35*, 172 – 174.
[84] S. R. Raghavan, H. J. Walls, S. A. Khan, *Langmuir* **2000**, *16*, 7920 – 7930.
[85] I. Ametov, C. A. Prestidge, *J. Phys. Chem. B* **2004**, *108*, 12116 – 12122.
[86] J. J. Valle-Delgado, J. A. Molina-Bolivar, F. Galisteo-Gonzalez, M. J. Galvez-Ruiz, A. Feiler, W. W. Rutland, *J. Chem. Phys.* **2005**, *123*, 034708.
[87] T. F. Tadros, J. Lyklema, *J. Electroanal. Chem.* **1968**, *17*, 267 – 271.
[88] P. G. Hartley, I. Larson, P. J. Scales, *Langmuir* **1997**, *13*, 2207 – 2214.
[89] J. J. Adler, Y. I. Rabinovich, B. M. Moudgil, *J. Colloid Interface Sci.* **2001**, *237*, 249 – 258.
[90] G. Vigil, Z. H. Xu, S. Steinberg, J. Israelachvili, *J. Colloid Interface Sci.* **1994**, *165*, 367 – 385.
[91] B. V. Zhmud, A. Meurk, L. Bergstrom, *J. Colloid Interface Sci.* **1998**, *207*, 332 – 343.
[92] A. C. J. H. Johnson, P. Greenwood, M. Hagstrom, Z. Abbas, S. Wall, *Langmuir* **2008**, *24*, 12798 – 12806.
[93] R. F. Considine, C. J. Drummond, *Langmuir* **2001**, *17*, 7777 – 7783.
[94] M. Kagawa, Y. Syono, Y. Imamura, S. Usui, *J. Am. Ceram. Soc.* **1986**, *69*, C-50 – C-51.
[95] J. Riley, in *Colloid Science Principles, Methods and Applications* (Ed.: T. Cosgrove), Blackwell Publishing, Oxford **2005**, pp. 14 – 35.
[96] S. N. Kalmykov, E. V. Zakharova, A. P. Novikov, F. M. Myasoedov, S. Utsunomiya in *Actinide Nanoparticle Research* (Eds.: S. Kalmykov, M. A. Denecke), Springer, Berlin, New York **2011**, pp. 361 – 375.
[97] N. Kozai, T. Ohnuki, T. Iwatsuki, *Water Res.* **2013**, *47*, 1570 – 1584.
[98] S. Wold, T. E. Eriksen, *Appl. Clay Sci.* **2003**, *23*, 43 – 50.
[99] P. Kunze, H. Seher, W. Hauser, P. J. Panak, H. Geckeis, T. Fanghänel, T. Schafer, *J. Contam. Hydrol.* **2008**, *102*, 263 – 272.
[100] T. Schäfer, F. Huber, H. Seher, T. Missana, U. Alonso, M. Kumke, S. Eidner, F. Claret, F. Enzmann, *Appl. Geochem.* **2012**, *27*, 390 – 403.
[101] R. H. Moench, *Am. Mineral.* **1962**, *47*, 26 – 33.
[102] M. Amme, T. Wiss, H. Thiele, P. Boulet, H. Lang, *J. Nucl. Mater.* **2005**, *341*, 209 – 223.
[103] J. D. Bauer, S. Labs, S. Weiss, L. Bayarjargal, W. Morgenroth, V. Milman, A. Perlov, H. Curtius, D. Bosbaxh, H. Zänker, B. Winkler, *J. Phys. Chem. C* **2014**, *118*, 25141 – 25149.
[104] J. Janeczek, R. C. Ewing, *J. Nucl. Mater.* **1992**, *190*, 157 – 173.
[105] V. Pointeau, A. P. Deditius, F. Miserque, D. Renock, U. Becker, J. Zhang, N. Clavier, N. Dacheux, C. Poinssot, R. C. Ewing, *J. Nucl. Mater.* **2009**, *393*, 449 – 458.
[106] S. Labs, C. Hennig, S. Weiss, H. Curtius, H. Zänker, D. Bosbach, *Environ. Sci. Technol.* **2014**, *48*, 854 – 860.
[107] V. Robit – Pointeau, C. Poinssot, P. Vitorge, B. Grambow, D. Cui, K. Spahiu, H. Catalette, *Mater. Res. Soc. Symp. Proc.* **2006**, *932*, 489 – 496.
[108] S. Szenknect, D. T. Costin, N. Clavier, A. Mesbah, C. Poinssot, P. Vitorge, N. Dacheux, *Inorg. Chem.* **2013**, *52*, 6957 – 6968.
[109] A. P. Deditius, S. Utsunomiya, R. C. Ewing, *Chem. Geol.* **2008**, *251*, 33 – 49.
[110] X. Guo, S. Szenknect, A. Mesbah, S. Labs, N. Clavier, C. Poinssot, S. V. Ushakov, H. Curtius, D. Bosbach, R. C. Ewing, P. C. Burns, N. Dacheux, A. Navrotsky, *Proc. Natl. Acad. Sci. USA* **2015**, *112*, 6551 – 5.
[111] A. Mesbah, S. Szenknect, N. Clavier, J. Lozano-Rodriguez, C. Poinssot, C. Den Auwer, R. C. Ewing, N. Dacheux, *Inorg. Chem.* **2015**, *54*, 6687 – 6696.

Received: November 10, 2015
Revised: February 26, 2016
Published online on April 21, 2016

 © 2016 The Authors. Published by Wiley-VCH Verlag GmbH & Co. KGaA, Weinheim